


Standard Article

J Vet Intern Med 2018;32:260–266

Contrast-Enhanced Ultrasound Examination for the Assessment of Renal Perfusion in Cats with Chronic Kidney Disease

E. Stock , D. Paepe, S. Daminet, E. Vandermeulen, L. Duchateau, J.H. Saunders*, and K. Vanderperren*

Background: Contrast-enhanced ultrasound examination (CEUS) is a functional imaging technique allowing noninvasive assessment of tissue perfusion. Studies in humans show that the technique holds great potential to be used in the diagnosis of chronic kidney disease (CKD). However, data in veterinary medicine are currently lacking.

Objectives: To evaluate renal perfusion using CEUS in cats with CKD.

Animals: Fourteen client-owned cats with CKD and 43 healthy control cats.

Methods: Prospective case-controlled clinical trial using CEUS to evaluate renal perfusion in cats with CKD compared to healthy control cats. Time-intensity curves were created, and perfusion parameters were calculated using off-line software. A linear mixed model was used to examine differences between perfusion parameters of cats with CKD and healthy cats.

Results: In cats with CKD, longer time to peak and shorter mean transit times were observed for the renal cortex. In contrast, a shorter time to peak and rise time were seen for the renal medulla. The findings for the renal cortex indicate decreased blood velocity and shorter total duration of enhancement, likely caused by increased vascular resistance in CKD. Increased blood velocity in the renal medulla has not been described before and may be because of a different response to regulatory factors in cortex and medulla.

Conclusions and Clinical Importance: Contrast-enhanced ultrasound examination was capable of detecting perfusion changes in cats with CKD. Further research is warranted to assess the diagnostic capabilities of CEUS in early stage of the disease process.

Key words: CKD; Contrast-enhanced ultrasound; Feline; Kidney.

Chronic kidney disease (CKD) is 1 of the most commonly diagnosed diseases in cats. The prevalence has been reported to be approximately 1–3% in the general feline population, even increasing to 30% in geriatric cats.^{1–3} Renal disease is reported to be the cause of death in 14–17% of geriatric cats.⁴ A primary, often unidentified trigger, initiates renal damage and nephron loss, which ultimately results in self-perpetuating renal injury and progressive renal disease.⁵ The most common histologic findings in cats with CKD are tubulointerstitial lesions such as tubular atrophy, interstitial inflammation, and fibrosis.⁶ Diagnosis at an early stage of the disease progress allows timely institution of supportive treatment and slows the disease progress.⁷ Prompt diagnosis remains challenging. The diagnosis

From the Department of Medical Imaging of Domestic Animals (Stock, Vandermeulen, Saunders, Vanderperren); the Small Animal Department, (Paepe, Daminet); and the Department of Comparative Physiology and Biometry, Faculty of Veterinary Medicine, Ghent University, Merelbeke, Belgium (Duchateau).

*Shared senior authorship.

This research was supported by the Special Research Fund of Ghent University, Belgium.

Corresponding author: E. Stock, Department of Medical Imaging of Domestic Animals, Faculty of Veterinary Medicine, Ghent University, Salisburylaan 133, 9820 Merelbeke, Belgium; e-mail: Emmelie.Stock@UGent.be

Submitted April 29, 2017; Revised August 25, 2017; Accepted October 11, 2017.

Copyright © 2017 The Authors. Journal of Veterinary Internal Medicine published by Wiley Periodicals, Inc. on behalf of the American College of Veterinary Internal Medicine.

This is an open access article under the terms of the Creative Commons Attribution-NonCommercial License, which permits use, distribution and reproduction in any medium, provided the original work is properly cited and is not used for commercial purposes.

DOI: 10.1111/jvim.14869

Abbreviations:

AUC	area under the curve
CEUS	contrast-enhanced ultrasound examination
CKD	chronic kidney disease
EDTA	ethylenediaminetetraacetic acid
FT	fall time
GFR	glomerular filtration rate
mTT	mean transit time
PE*	peak enhancement normalized to interlobar artery
PE	peak enhancement
ROI	region of interest
RT	rise time
sCr	serum creatinine
TTP	time to peak
UPC	urinary protein:creatinine ratio
USG	urine specific gravity
WiAUC	wash-in area under the curve
WiPI	wash-in perfusion index
WiR	wash-in rate
WoAUC	wash-out area under the curve
WoR	wash-out rate

most often is based on increases in serum urea and creatinine concentrations combined with low urine specific gravity. These changes unfortunately are only present when a substantial portion of renal function already has been lost. Measurement of glomerular filtration rate (GFR) provides more accurate assessment of renal function, but requires multiple blood samples, limiting its use in routine clinical practice.^{8,9} Therefore, the search for improved noninvasive methods for the diagnosis of early renal disease is still ongoing.

Renal function is closely related to renal perfusion. Therefore, evaluation of renal perfusion could yield valuable information about kidney function and thus

facilitate earlier diagnosis. Performing an accurate and noninvasive measurement of renal perfusion is challenging. Dynamic high-field magnetic resonance imaging, contrast-enhanced computed tomography, or renal scintigraphy can be used to assess renal perfusion. In practice, clinical application of these techniques is limited by relatively high costs, limited availability, long examination times, and exposure to ionizing radiation.^{10,11} Doppler ultrasound examination allows calculation of perfusion indices that provide information about vascular resistance. These indices are increased in animals with renal disease, but are relatively nonspecific because they are influenced by several nonrenal factors.^{12–14} Moreover, Doppler ultrasound examination is limited to evaluation of macroperfusion because low-velocity flow in smaller vessels cannot be assessed.¹²

Contrast-enhanced ultrasound examination (CEUS) is a functional imaging technique using microbubbles to enhance detection of tissue perfusion at the microvascular level. These bubbles are gas-filled spheres stabilized by an outer shell. They have a size similar to that of red blood cells and thus are restricted to the blood pool after IV injection. In cats, the literature currently is limited to the description of the normal perfusion pattern in healthy animals.^{15–17} In dogs, the perfusion pattern of focal mass lesions has been described, and quantitative CEUS in dogs with iatrogenically-induced hypercortisolism and ischemic renal disease has been described.^{18–20} Lower blood velocity was found in the dogs with ischemic renal disease, whereas an increase in renal blood volume was seen in dogs with hypercortisolism.^{19,20} Contrast-enhanced ultrasound examination has been shown to be a promising technique for the early diagnosis of renal disease in humans, but data on cats with renal disease are currently lacking.^{21,22}

Our aim was to evaluate the efficacy of CEUS in the diagnosis of CKD in cats. Our hypothesis was that CEUS would be a practical, noninvasive technique to detect perfusion changes in cats with CKD.

Materials and Methods

The study was performed with approval of the local ethical committee of the Faculty of Veterinary Medicine, Ghent University, Belgium and the deontological committee of the Belgian Federal Agency for the Safety of the Food Chain (EC2015-68). All owners gave their full informed consent to participate in the study.

Subjects

Fourteen client-owned cats with CKD and 43 healthy control cats were included. The diagnosis of CKD was made before inclusion and was based on the presence of compatible clinical signs and laboratory findings such as increased serum creatinine concentration ($>161.8 \mu\text{mol/L}$)²³ and decreased urine specific gravity (<1.035). Cats with clinically relevant concurrent systemic disease, hyperthyroidism, or urinary tract obstructions leading to postrenal azotemia were excluded. The cats with CKD were subdivided into 4 groups according to the classification of the International Renal Interest Society (IRIS).²⁴ Cats without clinically relevant abnormalities in history, on physical examination, thoracic radiographs, routine abdominal ultrasound examination, CBC, serum

biochemistry, and urinalysis were considered healthy. All medication or nutritional supplements, except for phosphorous binders in the CKD group, were withdrawn at least 14 days before inclusion.

Study Design

A thorough physical examination, including noninvasive measurement of blood pressure by Doppler ultrasonic technique and cervical palpation for scoring thyroid gland size (in cats >6 years), was performed.²⁵ Blood testing consisted of CBC and serum biochemistry, including total thyroxine (TT4) serum concentration in cats >6 years of age. Urinalysis included urine specific gravity (USG), sediment analysis (as previously described),²⁶ urinary protein/creatinine ratio (UPC), dipstick chemistry, and urine culture. Thoracic radiographs (left-to-right lateral and ventrodorsal projections) and complete abdominal ultrasound examination were performed.

CEUS Procedure

A 22-gauge indwelling catheter was placed in the cephalic vein.

The hair was clipped over the ventrolateral portion of the abdomen and coupling gel was applied to the skin. The ultrasound examinations were performed with the cat manually restrained in dorsal recumbency. The kidney of interest was centered on the screen and was imaged in a longitudinal plane using dual-screen (simultaneous display of conventional B-mode and contrast-mode images). The transducer was manually positioned during each imaging procedure and was maintained at the same position during CEUS.

The contrast agent,^a 0.05 mL/kg, was injected IV (bolus injection over approximately 3 seconds) followed by injection of a 1.5 mL saline bolus. A 3-way stopcock was used to avoid any delay between injection of contrast agent and saline. The same person performed the injection in a standardized way in all cats. Three injections of contrast were performed: 2 for the left kidney and 1 for the right kidney. The first injection was not used for further analysis, because it results in lower enhancement compared to the second and third injection.²⁷ Between subsequent injections, to avoid artifacts, remnant microbubbles were completely destroyed by setting the acoustic power at the highest level and scanning the caudal aspect of the abdominal aorta for approximately 2 minutes.

All examinations were performed using a linear transducer of 12–5 MHz on a dedicated machine^b with contrast-specific software. Basic technical parameters were a single focus placed under the kidney, persistency off, mechanical index 0.09, high dynamic range setting (C50), timer started at the beginning of the injection, gain (85%, corresponding to a nearly dark/anechoic image before contrast agent administration). The settings were repeated during each injection. All studies were digitally registered as a movie clip at a rate of 9 frames per second, for 90 seconds.

The clips were analyzed using specialized computer software^c for objective quantitative analysis. Six regions-of-interest (ROIs) were manually drawn: 3 in the renal cortex, 2 in the renal medulla, and 1 on an interlobar artery. The ROIs were similar in size and drawn at the same depth for every region. For every ROI, the software determined mean pixel intensity and created a time-intensity curve. Time-intensity curves were analyzed for peak enhancement (PE), wash-in area under the curve (WiAUC), rise time (RT), mean transit time (mTT), time to peak (TTP), wash-in rate (WiR), wash-in perfusion index (WiPI; WiAUC/RT), wash-out area under the curve (WoAUC), total area under the curve (AUC), fall time (FT), and wash-out rate (WoR). Parameters related to blood volume are PE, WiAUC, WoAUC, and AUC. The PE corresponds to the maximum contrast medium signal

intensity. The WiAUC is calculated as the sum of all amplitudes inside the range from the beginning of the curve up to the TTP. Similarly, WoAUC corresponds to the sum of all amplitudes inside the range from the TTP to the end of the descending curve. The other parameters (i.e., RT, mTT, TTP, WiR, WiPI, FT, WoR), are related to blood velocity. The WiR and WoR represent the maximum and minimum slopes of time-intensity curve. The RT corresponds to the time interval between the first arrival of contrast and the time of peak intensity. The FT, on the other hand, is the duration of contrast wash-out. Mean transit time is the mean duration of complete contrast medium perfusion. The perfusion parameters are illustrated in Figure 1. The values for the 3 ROIs in the renal cortex and the 2 ROIs in the renal medulla were averaged. Peak enhancement and WiAUC for the cortex and medulla were normalized to the values obtained for the interlobar artery.

Statistical Analysis

Statistical analyses were performed using statistical software.^d A linear mixed model with cat as random effect and health status (CKD/healthy) as categorical fixed effect was used. Age group also was incorporated in the model as a categorical fixed effect to adjust for age between CKD and healthy cats. Age groups were defined as: group 1 (1–3 years), group 2 (3–6 years), group 3 (6–10 years), and group 4 (>10 years). Correlations between perfusion parameters and renal size, IRIS stage, serum creatinine concentration (sCr), USG, and UPC were calculated for the renal cortex and medulla using Spearman correlation coefficients (ρ). A difference was considered statistically significant if $P < 0.05$.

Results

Breed distribution consisted of 9 domestic short- or long-haired cats and 5 pure-bred cats (2 Ragdoll cats, 2 Bengals, and 1 British Shorthair) for the group of cats with CKD and 41 domestic short- or long-haired cats and 2 pure-bred cats (2 Ragdoll cats) for the healthy cats. The mean \pm standard deviation age for the CKD group was 9.3 ± 5.2 years, and 6.5 ± 3.9 years for the healthy group. The mean \pm standard deviation body weight for the CKD group was 4.2 ± 1.1 kg, and for the healthy group 4.0 ± 0.7 kg. Six cats had IRIS stage 2 CKD, 1 of them was proteinuric (UPC > 0.4). Eight

cats had IRIS stage 3 CKD, of which 2 cats had proteinuria.

Systolic blood pressure, sCr, serum urea concentration, USG, and UPC are summarized in Table 1.

All healthy cats had normal size and appearance of their kidneys on B-mode ultrasonography. For the CKD group, renal size was <3.0 cm for 1 or both kidneys in 6 cats, 7 cats had segmental cortical lesions in 1 or both kidneys, an irregular outline for 1 of both kidneys was observed in 10 cats, and corticomedullary definition was decreased in all cats. One cat had mild unilateral pyelectasia, and another cat had mild bilateral pyelectasia, without signs of ureteral obstruction. A single large cyst deforming the renal cortex was present in 1 cat, whereas few small cortical cystic lesions were detected in both kidneys in another, domestic short-haired cat. None of the cats was diagnosed with polycystic kidney disease.

The contrast agent and the imaging procedure were well tolerated by all cats and no adverse effects were noticed.

Qualitative analysis of the CEUS images showed heterogeneous cortical enhancement in all cats with segmental cortical lesions (Fig 2).

Quantitative CEUS showed significant differences between CKD and healthy cats in several perfusion parameters for the renal cortex and medulla (Table 2 and Fig 2). The mTT for the renal cortex, a parameter for mean duration of complete contrast medium perfusion, was approximately 4 seconds shorter in cats with CKD compared to healthy cats ($P = 0.028$). The TTP for the cortex was longer in the CKD group ($P = 0.003$). In contrast, for the medulla, the TTP decreased for the cats with CKD ($P = 0.003$), associated with a shorter RT ($P = 0.001$) and FT ($P = 0.04$) (Figs 3 and 4).

For the renal cortex and medulla, significant correlations were present between the mTT and TTP and IRIS stage, and renal size. Additionally, significant correlations were identified between the RT for the renal medulla and sCr, IRIS stage, USG, and renal size. For the renal medulla, mTT and TTP also were significantly correlated to sCr, USG, and renal size. Urine specific gravity was significantly correlated to medullary RT, mTT and TTP and to cortical peak enhancement

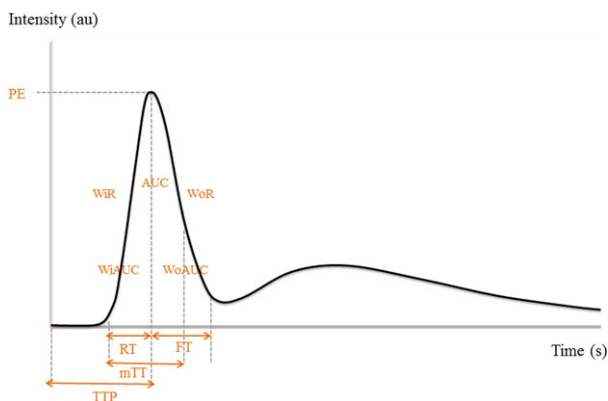


Fig 1. Typical time-intensity curve obtained after bolus injection of ultrasound contrast agent, illustration of the perfusion parameters. Time in second (s) is displayed on the horizontal axis and the intensity in arbitrary units (au) on the vertical axis.

Table 1. Baseline characteristics for CKD and healthy cats presented as mean \pm standard deviations.

Variables	Control group (n = 43)	CKD group (n = 14)	P-value
Blood pressure (mmHg)	144.3 \pm 13.5	141.0 \pm 38.7	0.632
sCr (μ mol/L)	110.4 \pm 19.5*	278.1 \pm 61.0*	<0.001
Serum urea (mmol/L)	8.2 \pm 1.5*	18.8 \pm 4.6*	<0.001
USG	1.048 \pm 0.004*	1.021 \pm 0.013*	<0.001
UPC	0.13 \pm 0.11*	0.34 \pm 0.33*	0.004

sCr, serum creatinine concentrations; USG, urine specific gravity; UPC, urinary protein:creatinine ratio. *significant difference.

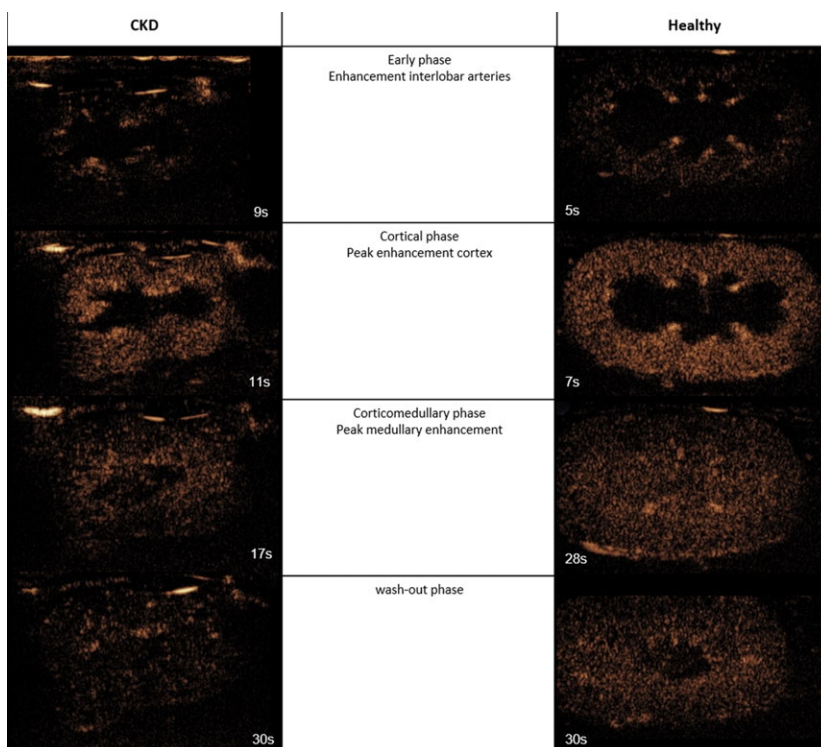


Fig 2. Representative serial contrast ultrasound images in a healthy cat (right) and a cat suffering from chronic kidney disease (left). The arrival of contrast agent in the renal cortex is delayed in cats with CKD; moreover, the duration of enhancement is shorter compared to healthy cats.

normalized to the interlobar artery. Additionally, a significant correlation was present for the cortical PE* and IRIS stage. Spearman correlation coefficients and *P*-values are summarized in Tables 3 and 4.

Discussion

Histologic studies in human and rodent kidneys have shown that tubulointerstitial lesions are associated with damage to the renal arterioles and arteries, and distortion and loss of peritubular capillaries.²⁸ Tubulointerstitial fibrosis impairs renal blood flow and increases renal vascular resistance.^{28,29} Renal capillary rarefaction is considered a central mechanism in initiation and progression of CKD in people and rodents.^{30,31} Moreover, the renin-angiotensin system is activated in CKD leading to higher renal tissue concentrations of angiotensin II compared to plasma concentrations. Because angiotensin II is a potent vasoconstrictor, the combination of these changes is likely to decrease renal blood flow in patients with CKD, resulting in decreased blood volume and velocity. A recent study using computed tomography angiography to evaluate renal blood volume and vascular anatomy in people showed a 41% decrease in renal cortical blood volume in patients with CKD compared to healthy subjects. The patients with CKD also had decreased luminal diameters of segmental arteries. Moreover, cortical renal blood volume decreased during progression of CKD and was correlated with a decrease

in GFR.³¹ Medullary blood volume was more variable and did not correlate with GFR.³¹

The most striking findings of our study were shorter mTT time, indicating shorter enhancement, and increased TTP in the renal cortex. The longer TTP suggests decreased blood velocity. These findings correspond to previous studies in human medicine, in which decreased TTP also was described in patients with CKD of various origin and in patients with diabetic nephropathy.^{32,33} Decreased TTP also was an early finding in dogs in which ischemic renal disease was induced by placing an ameroid constrictor around the renal artery.²⁰

The PE, a parameter for the intensity of enhancement, reflects the blood volume entering the kidney and hence is expected to be decreased in patients with CKD. Previous studies using CEUS in humans with CKD reported a decrease in PE^{21,22,32,33}; however, a significant decrease in PE was not identified in our study. Nevertheless, close inspection of the results in these studies shows that a great degree of overlap in PE is present for patients with CKD and healthy subjects.^{21,22,32,33} Relatively few patients with CKD were included in our study and larger numbers of cats are needed to determine if significance can be achieved. Moreover, PE is known to suffer from inherently high variability, because it is susceptible to many influencing factors.^{34,35} Variation may be attributed to the contrast agent itself (amount and physical properties of the

Table 2. Mean \pm standard deviation values of renal perfusion parameters for cats suffering from CKD and healthy cats.

Variable, by location	CKD	Healthy	P-value
Renal cortex			
PE	1635.12 \pm 1008.71	1779.16 \pm 991.75	0.643
PE*	19.24 \pm 14.82	27.72 \pm 13.18	0.065
WiAUC	2751.49 \pm 1442.52	2869.57 \pm 1418.18	0.791
RT	3.01 \pm 0.45	2.77 \pm 0.39	0.068
mTT	17.63 \pm 6.06	21.84 \pm 5.97	0.028
TTP	8.75 \pm 1.09	7.71 \pm 1.05	0.003
WiR	800.61 \pm 605.85	904.15 \pm 595.68	0.580
WiPI	1000.53 \pm 615.84	1089.36 \pm 605.45	0.640
WoAUC	3606.29 \pm 1824.25	3830.47 \pm 1793.46	0.690
AUC	6357.95 \pm 3262.09	6700.00 \pm 3207.05	0.733
FT	4.12 \pm 0.75	3.83 \pm 0.72	0.199
WoR	523.94 \pm 444.40	638.30 \pm 437.05	0.405
Renal medulla			
PE	208.71 \pm 762.21	276.83 \pm 649.58	0.766
PE*	3.65 \pm 2.62	3.02 \pm 2.36	0.433
WiAUC	1653.36 \pm 1307.00	1892.97 \pm 1133.85	0.542
RT	11.23 \pm 5.43	16.69 \pm 4.66	0.001
mTT	50.48 \pm 105.29	111.03 \pm 91.08	0.060
TTP	20.16 \pm 6.21	27.37 \pm 5.38	0.003
WiR	4.69 \pm 648.95	93.23 \pm 552.73	0.649
WiPI	130.85 \pm 466.66	172.68 \pm 397.51	0.765
WoAUC	2934.74 \pm 1979.94	3519.01 \pm 1970.38	0.387
AUC	4570.11 \pm 3449.17	5446.80 \pm 3065.60	0.404
FT	23.25 \pm 14.07	32.05 \pm 12.46	0.043
WoR	0.00 \pm 528.36	70.26 \pm 462.17	0.631

PE, peak enhancement; PE* normalized PE; WiAUC, wash-in area under the curve; RT, rise time; mTT, mean transit time; TTP, time to peak; WiR, wash-in rate; WiPI, wash-in perfusion index; WoAUC, wash-out area under the curve; AUC, total area under the curve; FT, fall time; WoR, wash-out rate. Values in bold represent significant differences between CKD and healthy cats.

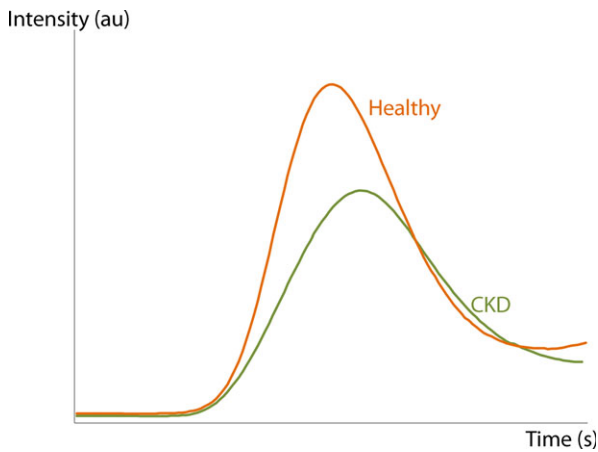


Fig 3. Mean time-intensity curves calculated for the renal cortex of healthy cats (orange) and cats with CKD (green) for the first 15 seconds after contrast injection, illustrating a delayed time to peak and a shorter mean transit time in cats suffering from CKD. The time in seconds (s) is displayed on the horizontal axis, the intensity in arbitrary units (au) on the vertical axis.

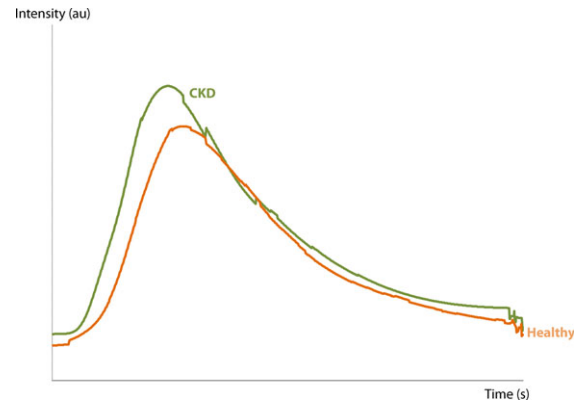


Fig 4. Mean time-intensity curves calculated for the renal medulla of healthy cats (orange) and cats with CKD (green) during 90 seconds after contrast injection, illustrating a shorter time to peak and short rise time for cats suffering from CKD. The time in seconds (s) is displayed on the horizontal axis, the intensity in arbitrary units (au) on the vertical axis.

Table 3. Correlations between IRIS stage, renal size, USG, and renal perfusion parameters for the renal cortex.

Variable pair	ρ (P)
IRIS stage – mTT	–0.29 (0.03)
IRIS stage – TTP	0.32 (0.02)
IRIS stage – PE*	–0.37 (0.005)
Renal size – mTT	0.30 (0.02)
Renal size –TTP	–0.30 (0.02)
USG – PE*	0.10 (0.43)

Table 4. Correlations between IRIS stage, renal size, USG, and renal perfusion parameters for the renal medulla.

Correlation	ρ (P)
sCr – mTT	–0.38 (0.004)
sCr – TTP	–0.43 (0.001)
sCr – RT	–0.46 (0.003)
IRIS stage – mTT	–0.38 (0.005)
IRIS stage – TTP	–0.47 (0.003)
IRIS stage – RT	–0.41 (0.002)
Renal size – mTT	0.43 (0.001)
Renal size –TTP	0.33 (0.01)
Renal size – RT	0.41 (0.001)
USG –mTT	0.45 (0.005)
USG – TTP	0.37 (0.006)
USG – RT	0.31 (0.02)

microbubbles), uncontrollable patient factors such as blood pressure, heart rate, filtration of the bubbles by the lungs, phagocytosis of bubbles by the reticuloendothelial system, and the manual injection procedure itself. Using controlled injection systems or continuous infusion of contrast agent, followed by flash-replenishment kinetics may improve the diagnostic accuracy of the technique.^{34,35}

Changes in AUC also have been described in humans with CKD, whereas no significance was obtained in our study. Both an increase and a decrease in AUC have been described in people with CKD. An increase in AUC was observed in early stage diabetic nephropathy, whereas a decrease was noticed in advanced stages.³³ An increase in AUC was reported in 41 humans with CKD, whereas a decrease was reported in a study of dogs with iatrogenic ischemic renal disease.^{20,21} The variable effects on AUC may be explained by the fact that AUC is influenced by PE, as well as the slope of the time-intensity curve. The AUC actually is composed of 2 parts: an initial part relating to inflow of contrast and a descending part related to the outflow of contrast medium. Moreover, AUC may be influenced by the stage and progression of CKD.

The decreased TTP and RT for the renal medulla in patients with CKD in our study were not completely expected. Only 1 study has described CEUS of the medulla in people with CKD. In the study of humans, findings for the medulla paralleled those of the cortex, showing delayed time to peak.³² Still, the vascular anatomy and physiology of the renal medulla differ substantially from those of the cortex. The renal medulla makes up <30% of the total renal volume but only receives 10% of the total renal blood flow. Additionally, local differences are described for the outer and inner medulla, with the latter being less perfused. Vasoactive regulatory factors have different effects on cortical and medullary blood flow. The medulla is relative insensitive to vasoconstriction.³⁶ Therefore, locally increased blood velocity could be present in the medulla in cats with CKD. However, additional studies are needed to confirm this finding and further investigate the underlying pathophysiology.

We found significant correlations between time-based perfusion parameters and sCr, IRIS stage, USG, UPC, and renal size. However, correlation coefficients were low and did not exceed 0.50 in most cases. The highest correlation coefficient was observed for UPC and TTP for the renal medulla. Similarly low, but significant correlation coefficients are described in 2 studies of humans. Correlation coefficients of 0.26–0.40 between the slope of the ascending and descending parts of the time-intensity curve and sCr-based estimated GFR have been observed.³² Additionally, a significant correlation was present between PE and estimated GFR ($r = 0.27$).³² Similarly, a correlation ($r = 0.47$) between AUC and GFR measured by radionuclide clearance techniques has been described in people with diabetic nephropathy.³³ Moreover, the correlations calculated in our study of cats are based on a small number of animals and therefore should be interpreted with caution.

The IRIS staging system is routinely used to facilitate monitoring, treatment, and estimating prognosis in dogs and cats with CKD. We investigated if differences in CEUS parameters could be identified among different IRIS stages. As described above, this goal was limited by the low number of cats. The severity of tubular degeneration, interstitial inflammation, fibrosis, and

glomerulosclerosis was significantly greater in later stages compared to earlier stages of CKD in cats.³⁷

We determined CEUS perfusion parameters in a large population of healthy cats. Previous studies performing CEUS in healthy cats only included small numbers of cats (8–10); moreover, only young cats were included. Additionally, sedation, anesthesia, or both were used in these studies, likely influencing renal perfusion.^{15–17} In addition to these issues, comparison of perfusion variables among studies is not possible because the injection procedure, contrast agent, machine settings, and software all influence the type of perfusion parameters calculated and their values. Time to peak is the most consistently calculated parameter in CEUS studies. The TTP in our study is in the same range as the TTP described in 1 study of cats,¹⁷ whereas it is substantially shorter compared to the results in another study of cats.¹⁶ Time to peak is largely influenced by the injection procedure and the sedation or anesthesia used.

In conclusion, our findings in a small cohort of cats with CKD are encouraging with respect to the use of CEUS to evaluate renal perfusion in cats. A decrease in blood velocity was detected for the renal cortex whereas increased blood velocity was present in the renal medulla. The enhancement of the renal cortex was found to be of shorter duration in cats with CKD (decreased mTT). However, no significant changes could be detected in parameters representing the blood volume. Additional studies are necessary to evaluate the added value of CEUS in the diagnosis of early, nonazotemic CKD in cats.

Footnotes

- ^a Sonovue[®], Bracco, Milan, Italy
 - ^b iU22, Philips, Amsterdam, The Netherlands
 - ^c VueBox[®], Bracco Suisse SA, Geneva, Switzerland
 - ^d SAS version 9.4, SAS Institute Inc, Cary, North Carolina
-

Acknowledgments

The authors thank Bracco Suisse SA (Geneva, Switzerland) for their scientific support on the use of VueBox[®] and Medvet (Antwerp, Belgium) for the laboratory analyses.

Conflict of Interest Declaration: Authors declare no conflict of interest.

Off-label Antimicrobial Declaration: Authors declare no off-label use of antimicrobials.

References

1. Lund EM, Armstrong PJ, Kirk CA, et al. Health status and population characteristics of dogs and cats examined at private veterinary practices in the United States. *J Am Vet Med Assoc* 1999;214:1336–1341.

2. Lulich JP, Osborne CA, Obrien TD, et al. Feline renal-failure - questions, answers, questions. *Comp Cont Educ Pract* 1992;14:127–152.
3. Polzin DJ. Chronic kidney disease. In: Ettinger SJ, Feldman EC, eds. *Textbook of Veterinary Internal Medicine: Diseases of the Dog and the Cat*, 7th ed. Missouri: Saunders Elsevier; 2010:1990–2020.
4. O'Neill DG, Church DB, McGreevy PD, et al. Longevity and mortality of cats attending primary care veterinary practices in England. *J Feline Med Surg* 2015;17:125–133.
5. Jepson RE. Current understanding of the pathogenesis of progressive chronic kidney disease in cats. *Vet Clin North Am: Small Animal Practice* 2016;46:1015–1048.
6. Brown CA, Elliott J, Schmiedt CW, et al. Chronic kidney disease in aged cats: Clinical features, morphology, and proposed pathogenesis. *Vet Pathol* 2016;53:309–326.
7. Paepe D, Daminet S. Feline CKD: Diagnosis, staging and screening - what is recommended? *J Feline Med Surg* 2013;15 (Suppl 1):15–27.
8. Paepe D, Lefebvre HP, Concordet D, et al. Simplified methods for estimating glomerular filtration rate in cats and for detection of cats with low or borderline glomerular filtration rate. *J Feline Med Surg* 2015;17:889–900.
9. Finco DR, Brown SA, Vaden SL, et al. Relationship between plasma creatinine concentration and glomerular filtration rate in dogs. *J Vet Pharmacol Ther* 1995;18:418–421.
10. Herget-Rosenthal S. Imaging techniques in the management of chronic kidney disease: Current developments and future perspectives. *Semin Nephrol* 2011;31:283–290.
11. Daniel GB, Mitchell SK, Mawby D, et al. Renal nuclear medicine: A review. *Vet Radiol Ultrasoun* 1999;40:572–587.
12. d'Anjou MA, Penninck D. Kidneys and ureters. In: Penninck D, d'Anjou MA, eds. *Atlas of Small Animal Ultrasonography*, 2nd ed. Oxford: Wiley Blackwell; 2015:331–362.
13. Tipisca V, Murino C, Cortese L, et al. Resistive index for kidney evaluation in normal and diseased cats. *J Feline Med Surg* 2015;18:471–475.
14. Novellas R, de Gopegui RR, Espada Y. Increased renal vascular resistance in dogs with hepatic disease. *Vet J* 2008;178:257–262.
15. Schweiger H, Ohlerth S, Gerber B. Contrast-enhanced ultrasound of both kidneys in healthy, non-anaesthetized cats. *Acta Vet Scand* 2015;57:57–80.
16. Kinns J, Aronson L, Hauptman J, et al. Contrast-enhanced ultrasound of the feline kidney. *Vet Radiol Ultrasoun* 2010;51:168–172.
17. Leinonen MR, Raekallio MR, Vainio OM, et al. Quantitative contrast-enhanced ultrasonographic analysis of perfusion in the kidneys, liver, pancreas, small intestine, and mesenteric lymph nodes in healthy cats. *Am J Vet Res* 2010;71:1305–1311.
18. Haers H, Vignoli M, Paes G, et al. Contrast harmonic ultrasonographic appearance of focal space-occupying renal lesions. *Vet Radiol Ultrasoun* 2010;51:516–522.
19. Haers H, Daminet S, Smets PMY, et al. Use of quantitative contrast-enhanced ultrasonography to detect diffuse renal changes in Beagles with iatrogenic hypercortisolism. *Am J Vet Res* 2013;74:70–77.
20. Dong Y, Wang WP, Cao JY, et al. Quantitative evaluation of contrast-enhanced ultrasonography in the diagnosis of chronic ischemic renal disease in a dog model. *PLoS ONE* 2013;8:e70377.
21. Dong Y, Wang WP, Cao J, et al. Early assessment of chronic kidney dysfunction using contrast-enhanced ultrasound: A pilot study. *Brit J Radiol* 2014;87:1–7.
22. Hosotani Y, Takahashi N, Kiyomoto H, et al. A new method for evaluation of split renal cortical blood flow with contrast echography. *Hypertens Res* 2002;25:77–83.
23. Ghys LF, Paepe D, Duchateau L, et al. Biological validation of feline serum cystatin C: The effect of breed, age and sex and establishment of a reference interval. *Vet J* 2015;204:168–173.
24. IRIS kidney. International renal interest society (IRIS) [Internet]. IRIS staging of CKD; c2017 [cited 2017 April 07]. Available from: <http://www.iris-kidney.com>.
25. Boretti FS, Sieber-Ruckstuhl NS, Gerber B, et al. Thyroid enlargement and its relationship to clinicopathological parameters and T-4 status in suspected hyperthyroid cats. *J Feline Med Surg* 2009;11:286–292.
26. Paepe D, Verjans G, Duchateau L, et al. Routine health screening: Findings in apparently healthy middle-aged and old cats. *J Feline Med Surg* 2013;15:8–19.
27. Stock E, Vanderperren K, Haers H, et al. Quantitative differences between the first and second injection of contrast agent in contrast-enhanced ultrasonography of feline kidneys and spleen. *Ultrasound Med Biol* 2017;43:500–504.
28. Nangaku M. Chronic hypoxia and tubulointerstitial injury: A final common pathway to end-stage renal failure. *J Am Soc Nephrol* 2006;17:17–25.
29. Basile DP, Donohoe D, Roethe K, et al. Renal ischemic injury results in permanent damage to peritubular capillaries and influences long-term function. *Am J Physiol Renal Physiol* 2001;281:F887–F899.
30. Horbelt M, Lee SY, Mang HE, et al. Acute and chronic microvascular alterations in a mouse model of ischemic acute kidney injury. *Am J Physiol Renal Physiol* 2007;293:F688–F695.
31. von Stillfried S, Apitzsch JC, Ehling J, et al. Contrast-enhanced CT imaging in patients with chronic kidney disease. *Angiogenesis* 2016;19:525–535.
32. Tsuruoka K, Yasuda T, Koitabashi K, et al. Evaluation of renal microcirculation by contrast-enhanced ultrasound with sonazoid (TM) as a contrast agent. *Int Heart J* 2010;51:176–182.
33. Ma F, Cang YQ, Zhao BZ, et al. Contrast-enhanced ultrasound with SonoVue could accurately assess the renal microvascular perfusion in diabetic kidney damage. *Nephrol Dial Transpl* 2012;27:2891–2898.
34. Tang MX, Mulvana H, Gauthier T, et al. Quantitative contrast-enhanced ultrasound imaging: A review of sources of variability. *Interface Focus* 2011;1:520–539.
35. Hyvelin JM, Tardy I, Arbogast C, et al. Use of ultrasound contrast agent microbubbles in preclinical research recommendations for small animal imaging. *Invest Radiol* 2013;48:570–583.
36. Evans RG, Eppel GA, Anderson WP, et al. Mechanisms underlying the differential control of blood flow in the renal medulla and cortex. *J Hypertens* 2004;22:1439–1451.
37. McLeland SM, Cianciolo RE, Duncan CG, et al. A comparison of biochemical and histopathologic staging in cats with chronic kidney disease. *Vet Pathol* 2015;52:524–534.